JOURNAL OF MATERIALS SCIENCE 32 (1997) 4447–4453

Preparation of a pitch-based activated carbon with a high specific surface area

WENMING QIAO, LICHENG LING, QINGFANG ZHA, LANG LIU
Institute of Coal Chemistry, Chinese Academy of Sciences, P.O. Box 165, Taiyuan, Shanxi, 030001, Peoples Republic of China

Pitch based activated carbons (PAC) with a high specific surface area were produced by a direct chemical activation route in which oxidative stabilized pitch derived from ethylene tar oil was reacted with potassium hydroxide under various activation conditions. It was found that PACs with a surface area of around 2600–3600 $m^2 g^{-1}$could be obtained under suitable activation conditions. N_2 adsorption (at 77 K) and X-ray photoelectron spectroscopy experiments showed that the PAC has a uniformly developed micropore structure and a narrow pore size distribution (radius 0.8–1.6 nm). Abundant oxygen-containing functional groups (such as C–OH, C–O–C, C=O, COOR etc.) were found to exist on its surface. Compared with a commercially available activated carbon (AC) and also a pitch based activated carbon fibre, PAC has a quicker adsorption–desorption velocity and a larger adsorptive capacity to benzene due to its higher surface area. Clear surface differences between PAC and AC were observed by transmission electron microscopy.

1. Introduction

Granular activated carbons (AC) made from coal or coconut shells have been of commercial interest for many years and are extensively used in modern industry [1–5]. However, in general these activated carbons that have a low surface area and poor adsorption properties cannot be applied to industries, such as environmental protection and medicine. Thus, high performance adsorbents are required. Recently, activated carbon fibre (ACF), which has a higher surface area and larger adsorption capacity than AC, has been developed and applied in some fields, however its widespread use has been limited by cost considerations [6, 7].

Pitch based activated carbons with high surface areas may offer a solution to this problem, since the pitch used as a raw material is cheaper than fibre, and it has a good adsorption performance [8, 9].

It has been reported that activated cokes with high Brunauer–Emmett–Telher (BET) surface area ($> 2500 m^2 g^{-1}$) could be obtained by a direct chemical activation using potassium hydroxide as the activation agent. This material has been used in fields as diverse as methane storage, municipal water treatment, catalysts and as a catalyst support (8–16). Recently, this type of activated carbon (called Maxsorb) has been commercially produced in Japan [17]. However the optimal preparation route, the physico-chemical structures and adsorption–desorption properties of this high performance activated carbon still remain to be fully elucidated.

In this study, oxidative stabilized pitch derived from ethylene tar oil was chosen as the starting material to prepare pitch based activated carbon (PAC) with a high specific surface area using potassium hydroxide as the activation agent. Various preparation conditions for the PAC were investigated, in detail and preliminary investigations on the surface structure and adsorption properties of this material were undertaken.

2. Experimental procedure

2.1. Preparation of PAC

The presence of inorganic impurities, such as ash, can influence the adsorption behaviour of activated carbon in aqueous solutions because they can affect its electrokinetic properties [18]. Ethylene-tar-oil derived pitch with a very low ash content of 0.04 wt%, is ideally suited to the preparation of high performance activated carbon, and its basic properties are summarized in Table I.

PAC was prepared through the following processes: the pitch was pulverized to the required size and was subsequently oxidatively stabilized under a hot air flow ($1 m^3 h^{-1}$) at a heating rate of $2 °C min^{-1}$ up to 320 °C. This was followed by the KOH activation at 400–1000 °C for 30–120 min under a nitrogen flow with a heating rate of $10 °C min^{-1}$. The activation was performed on KOH and pitch samples mixed at a certain ratio. Finally the products were washed with dilute HC1 and water to remove any unreacted KOH and salts formed during the activation.

2.2. Nitrogen adsorption isotherm of PAC

The nitrogen adsorption isotherm was measured using a ASAP2000 adsorption apparatus (Micrometics

TABLE I Basic properties of pitch derived from ethylene tar oil

Elemental analysis (wt %)			C/H (atom)	Ash (wt %)	Pynidine insoluble (wt %)	Softening point (°C)
C	H	O				
93.33	5.21	1.41	1.49	0.04	11.10	250

Comp.) at 77 K. The surface area and pore structure of PAC was calculated using the BET equation and methods [19], based on nitrogen adsorption.

2.3. Transmission electron microscopy

The surface structures of PAC and AC were probed by transmission electron microscopy (TEM) performed on a JOEL 100CX II microscope.

2.4. X-ray photoelectron spectroscopy of PAC

The X-ray photoelectron spectroscopy (XPS) method can be used to investigate chemical structures of carbonaceous materials [20–24]. XPS measurements were performed using a PHI-5300 ESCA (Perkin-Elmer) operated at 12.5 kv and 20 mA to produce Mg K_α X-rays with an energy of 1256.3 ev. Measurements were performed in a residual vacuum of 1.333×10^{-6} Pa. The data was collected with the analyser in fixed transmission mode and normal to the plane of the sample. All the measured peaks have been charge referenced to the major C–C/C–H 1s peak at 284.71 ev. An analyser pass energy of 85.45 ev has been used to record broad scan spectra from which surface composition data have been calculated. A pass energy of 71.55 ev has been used to record high resolution carbon 1s peak envelopes to derive chemical shift information. Surface compositions have been calculated using the areas of the respective photoelectron peaks after subtraction of a Shirley-type background. The sampling depth of the technique is approximately 5 nm. The photoelectron peak broadening due to X-ray line shape effects has been removed from the high-energy resolution carbon 1s spectra using in-house software on a professional microcomputer 7500.

2.5. The adsorption–desorption characteristics of PAC

The adsorption–desorption characteristics of PAC was measured through weight gain using a Dupont Instruments Series 99 Thermal Analyser. A 50 mg sample was placed in a thermogravimetric balance, dried at 150 °C in a helium flow, which was followed by the adsorption of saturated benzene vapour (helium as carrier gas, the total flow rate was 20 ml min^{-1}) at 25 °C. The desorption of PAC after the benzene adsorption was carried out at 150 °C by using a helium flow rate of 37 ml min^{-1}. This process was recycled once to investigate its regeneration ability.

3. Results and discussion

3.1. Preparation of PAC

3.1.1. The effect of temperature on the activation process

Fig. 1 shows the effect of temperature on the activation process. The yield of the activated product decreased and its surface area increased steadly with an increase in the applied temperature. In the light of the corrosion to the stainless steel reactor, produced by the mild KOH a temperature of 900 °C was chosen for the activation experiments.

3.1.2. The effect of the oxidative stabilization temperature of the pitch

The effect of the oxidative stabilization temperature of the pitch on the activation results is shown in Fig. 2. Variation in the oxidative stabilization temperatures results in differences in the properties of the activated products at the same activation condition. With an increase in the oxidative stabilization temperature,

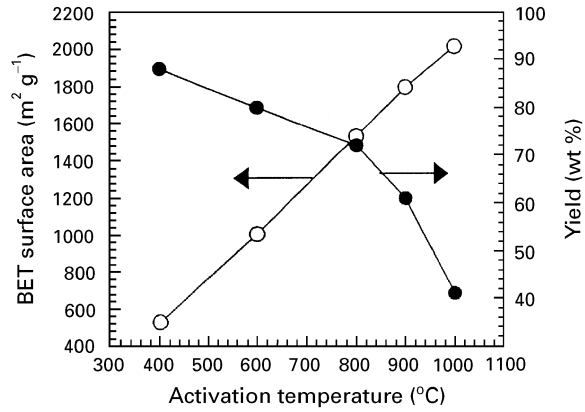

Figure 1 The effect of temperature on the activation process. Raw material : infusible pitch (74–100 um) an oxidative stabilization temperature of 260 °C; the activation time : 30 min; the ratio of KOH/pitch (wt/wt): 2.

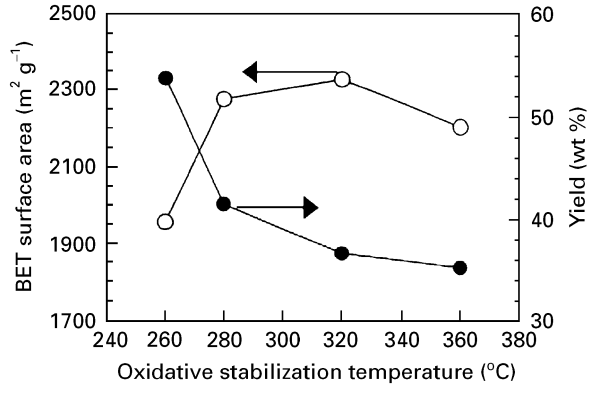

Figure 2 The effect of the oxidative stabilization temperature of the pitch on the activation process. Size of infusible pitch: 74–100 um; the activation time: 60 min; the ratio of KOH/pitch: 2. The O/C (wt/wt) of the pitch at oxidative stabilization temperatures of 260, 280, 320 and 360 °C: were 0.08, 0.10, 0.18, 0.19, respectively (measured by XPS).

a larger oxygen content was observed on the surface of the pitch [25]. The surface area initially increased with the increase in the oxidative stabilization temperature, reaching a maximum value of 2310 $m^2 g^{-1}$ at 320 °C, and then it decreased. This can be explained by the point that during the activation the KOH reacted with oxygen-containing functional groups to form organometallic salts of the type R–OK and R–COOK. The oxygen is provided by the alkali salts [26], used to promote the reaction between the carbonaceous material and KOH to create more micropore structures. The presence of potassium and oxygen in the structure of the carbonaceous materials can cause separation of the lamellea in the structure due to oxidation produced by crosslinking of carbon atoms. In addition the formation of functional groups on the edges of the lamellea may cause them to pucker out of the expected flat form. When the potassium salts are removed from the carbonaceous particle by leaching with water, the lamellea cannot return to their previous non-porous structure but instead remain apart to create the microporosity necessary for high surface area values [12]. The introduction of oxygen into the pitch during activation may partly break down the microporous structure of PAC due to its decomposition, which can result in a decrease in the surface area of the activated carbon.

The oxygen of the alkali can remove crosslinking, and thus stabilizing, carbon atoms in crystallites. Any potassium metal liberated at the reaction temperature may intercalate into the carbon and force apart the lamellea of the crystallite. The removal of potassium salts and carbon atoms from the internal volume of the carbon creates the microporosity of a new structure [12].

As shown in Fig. 2, the activation reaction of precarbonized carbonaceous materials is not favoured because of the growth in size of the constituent lamellea thus preventing significant movement to create microporosity and a significant removal of internal carbon atoms.

3.1.3. The effect of the KOH/pitch ratio

The effect of the KOH/pitch ratio on the activation process is shown in Fig. 3. The surface area steadily increased as the ratio increased from 0.5–4, while the yield decreased. The burn-off of excess PAC occurred when the ratio of KOH/pitch was high enough (6 : 1) but this resulted in some of the micropores being destroyed which in turn lead to lower surface area values.

3.1.4. The effect of activation times

The effect of activation times on the activation process is shown in Fig. 4. A similar effect to that observed for oxidative stabilization temperature and the KOH/pitch ratio on the activation was observed. The surface area initially increased reaching a maximum value of 2666 $m^2 g^{-1}$ after 60 min but it then decreased due to the excess burning of carbonaceous materials during the activation.

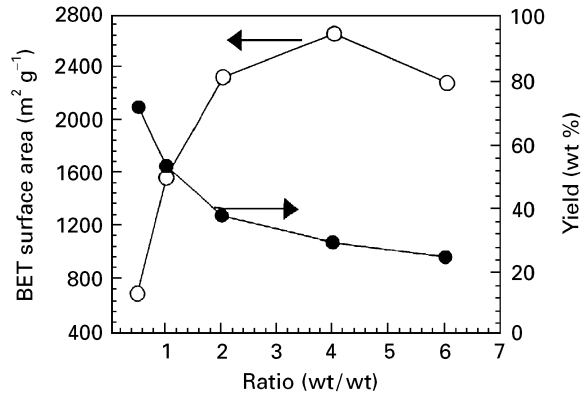

Figure 3 The effect of the KOH/pitch ratio on the activation process. Raw material: infusible pitch (74–100 um) an oxidative stabilization temperature of 320 °C; activation temperature: 900 °C; the activation time: 60 min.

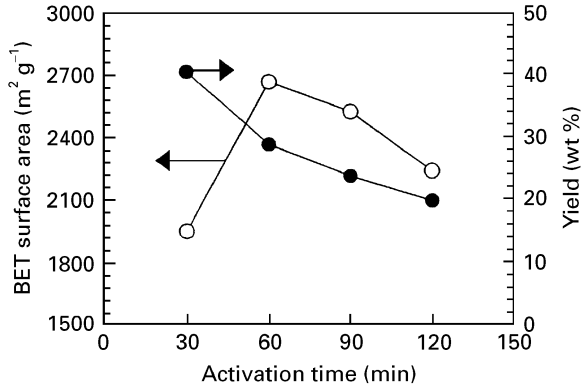

Figure 4 The effect of activation time on the activation process. Raw material: infusible pitch (74–100 um) an oxidative stabilization temperature of 320 °C; activation temperature: 900 °C; ratio of KOH/pitch: 4.

TABLE II The effect of the size of the raw material on the activation process

Size of raw material (um)	74–100	65–75	40–65
Yield (wt %)	28.8	24.7	20.5
BET surface area ($m^2 g^{-1}$)	2666	3021	3646
Adsorptive capacity to Iodine ($mg g^{-1}$)	2633	2905	3114

Raw material: infusible pitch at an oxidative stablization temperature of 320 °C; the activation temperature: 900 °C; the activation time : 60 min; the ratio of KOH/pitch: 4

3.1.5. The effect of the size of the raw materials

The effect of the size of the raw materials on the activation process is listed in Table II. The surface area continuously increased as the size of the raw material decreased. A maximum surface area of 3646 $m^2 g^{-1}$ can be obtained using raw materials with a size between 40–65 μm after the activation. It can be concluded that when the size of the infusible pitch decreased, its external surface increased thus

promoting the reaction with KOH, and also a larger external surface might contain more active sites for the activation.

The theoretical upper limit of the specific surface area for carbonaceous materials is 2622 $m^2 g^{-1}$, which is calculated using the single layer graphite structure [19]. However this upper limit need not necessarily apply in our case since activated carbons are non-graphitiziable carbons. The activated carbons are not composed of well crystallized graphites, but poorly crystalline micrographites. X-ray diffraction techniques showed that the cristallite size of the micrographites is less than 5 nm and the *c*-spacing is greater than that of graphite due to less alignment of the graphitic layers [27]. Thus, the micropore walls are produced from graphitic microcrystallites. The size, mutual orientation, and stacking of the micrographites are closely associated with the microporosity and the large surface area. Considering the above microcrystalline graphitic structures, the upper limit of 2622 $m^2 g^{-1}$ for the surface area does not apply to activated carbons, and a surface area of more than 3000 $m^2 g^{-1}$ is attainable [27].

3.2. Nitrogen adsorption isotherm

The nitrogen adsorption isotherms of the two PAC samples (i.e., PAC1 and PAC2, whose preparation conditions are shown in Fig. 3) are shown in Fig. 5, the data are summarized in Table III, and their pore size distributions are shown in Fig. 6.

Under a lower relative pressure ($P/P_0 < 0.25$), both PAC1 and PAC2 adsorb large nitrogen volumes (V_a) and the rate of increase of $V_a(R_{va})$ which increases as the relative pressure increases is also large. Compared with PAC2, PAC1 has a far larger V_a and R_{va}. This indicates that both PAC1 and PAC2 are micropore activated carbons with PAC1 having a much larger surface area which is mainly ascribed to a greater number of micropores [20, 21].

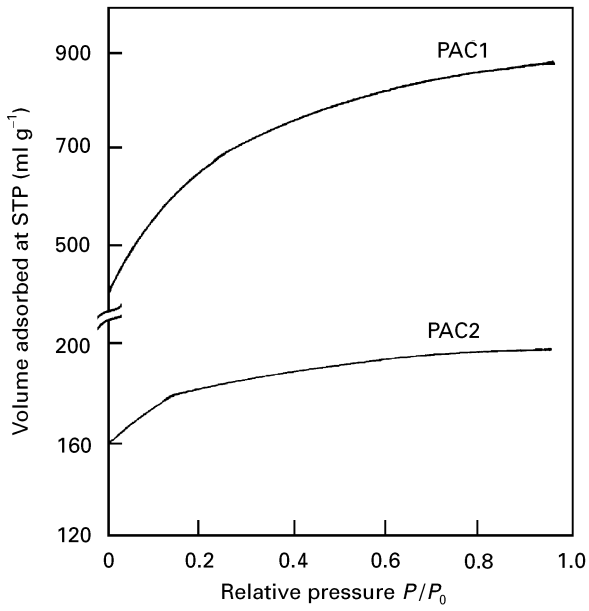

Figure 5 Nitrogen adsorption isotherms of two PACs.

TABLE III Summaries of nitrogen adsorption data of PACs

Sample	S_{BET} ($m^2 g^{-1}$)	S_{ext} ($m^2 g^{-1}$)	V_p ($cm^3 g^{-1}$)	V_{mic} ($cm^3 g^{-1}$)
PAC1	2666	353	1.543	1.375
PAC2	683	26	0.317	0.290

S_{ext}: nonmicropore surface area derived from the slope of the α s-plot at $\alpha_s > 1$ (not shown here)
V_P: total pore volume calculated from uptake on desorption branch at $P/P_0 = 0.95$
V_{mic}: micropore volume calculated from the α s-plot

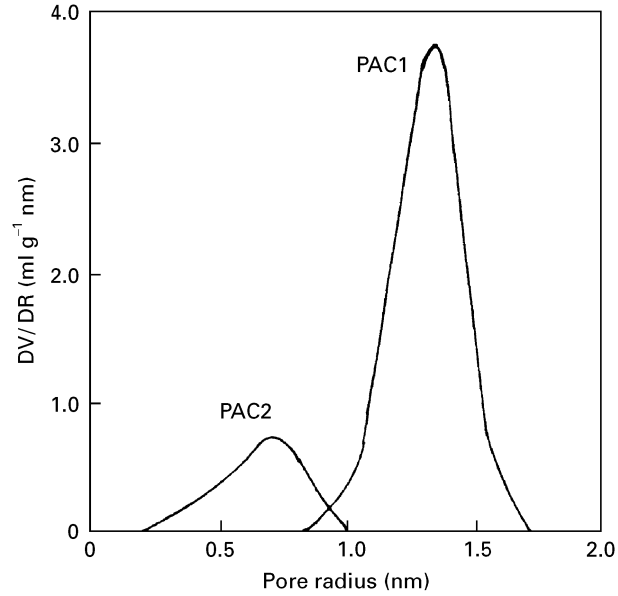

Figure 6 Pore size distributions of PACs.

Fig. 6 shows that the pore radius distribution of PAC1 is between 0.8–1.6 nm, whereas that of PAC2 between 0.5–0.8 nm. PAC1 has a narrow pore size distribution which is similar to that of PACF [28]. This implies that activated carbons containing more micropores and a slightly larger radius could be obtained.

3.3. TEM

It can be seen that PAC1 that has the high specific surface area of 2666 $m^2 g^{-1}$ area has a uniform surface structure (called a cage-like structure) [10, 11] consisting of a lot of micropores (Fig. 7a) and that an AC($S_{BET} \sim 1100\ m^2 g^{-1}$, produced by the Xin Hua Chemical factory, Xin Hua, China) possesses a rough surface, containing a considerable number of defects and a disordered pore structure (Fig. 7b). Thus, PAC has a larger specific surface area than does AC.

3.4. XPS

The surface chemical properties of activated carbons are related to the presence of chemical groups analogous to the functional groups of organic compounds, that affect in a decisive manner their ion-exchange, catalytic, electronic, and adsorptive properties [29]. Fig. 8 shows broad scan XPS spectra for PAC1. The

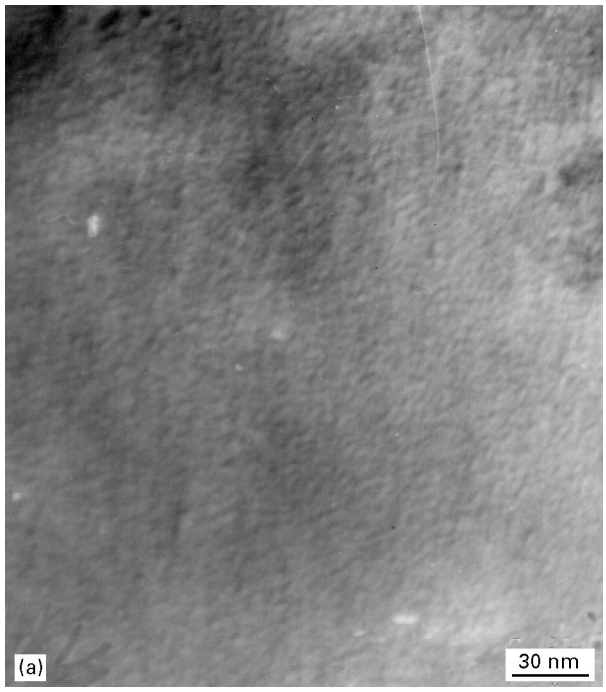

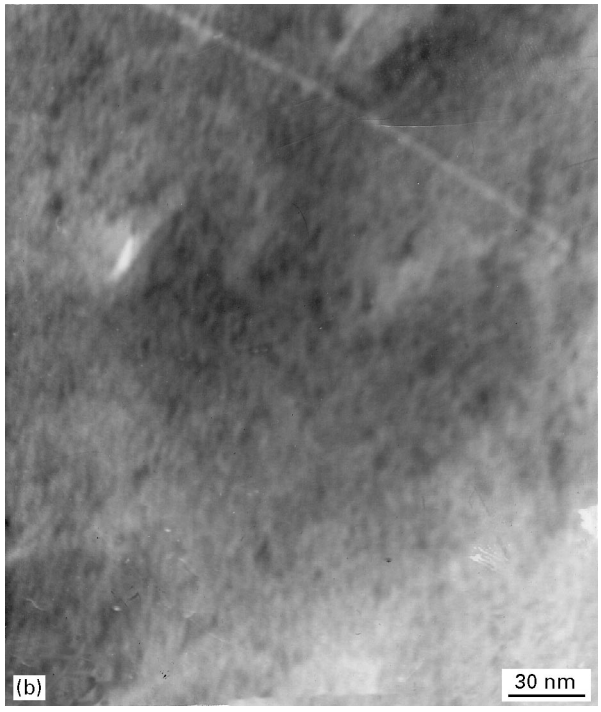

Figure 7 TEM images of (a) PAC1 and (b) AC.

elemental analysis data for sample PAC1 are listed in Table IV. High energy resolution carbon ls XPS and fitted-carbon ls XPS of PAC1 are shown in Figs 9 and 10, respectively.

From Fig. 8 and Table IV the elemental compositions of PAC1 consists of carbon, oxygen, hydrogen, and nitrogen, with carbon and oxygen having the largest concentrations. The surface oxygen content of PAC1 is greater than the average one, indicating that oxygen-containing functional groups formed on the surface of the PAC during the activation process although the mechanism of their formation is as yet unclear.

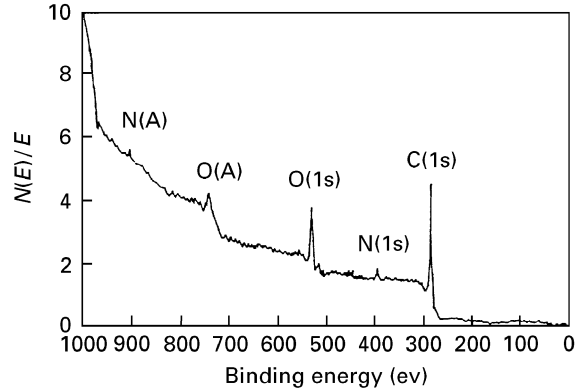

Figure 8 Broad scan XPS spectra for PAC1.

The major peak shown in Fig. 9 has been assigned a binding energy of 284.71 ev and has been used as a reference peak. This peak is, however, most probably attributable to both graphitic carbon ring structures and CHn and the difference in binding energy between these two forms is 0.2–0.23 ev, which is effectively beyond the resolution of the instrument. In addition, a series of peaks shifted to the higher binding energy side of the main peak are observed. These are shown, in greater detail in Fig. 10. Three peaks are observed, which occur at shifts of 1.58, 2.9 and 4.61 ev from the main peak. These have been tentatively attributed to C–O (ether/hydroxyl, 16.22%), C=O (carbonyl, 10.86%), and COOH (carboxylic, 8.07%) functionalities, respectively.

3.5. Adsorption and desorption properties

Fig. 11 (a and b) describes the adsorption–desorption behaviour of PAC1 to benzene vapour for comparison purposes the adsorption–desorption plots for PACF and AC are also depicted.

Compared with PACF and AC, PAC has a surprising adsorptive capacity to benzene. In the first run of the adsorption and desorption process, the maximum adsorptive capacity of PAC1 to benzene is $970\,mg\,g^{-1}$, but those of PACF and AC are $600\,mg\,g^{-1}$ and $375\,mg\,g^{-1}$, respectively. The slope of the adsorptive branch of PAC1 is steeper than those of PACF and AC, which means that PAC1 has the quickest adsorptive velocity. It should be noted that the adsorptive branch of PAC1 consists of two stages, namely a straight line and a curved line (parabola), and the former is similar to the adsorptive branch of PACF, but the latter is different, implying that PAC1 still contains a few micropores, in which the diffusion of benzene molecules is relatively difficult, which reduces their velocity. In addition PAC has a faster desorptive velocity than PACF and AC.

In the second cycle of adsorption and desorption (shown in Fig. 11a), the branches of the adsorption and desorption of PAC1 are similar to those in Fig. 11b, but the maximum adsorptive capacity of PAC1 to benzene decreases to $910\,mg\,g^{-1}$ or by 6%. Meanwhile the adsorptive capacity of AC decreases by 12%. These values indicate that PAC1 has

TABLE IV Elemental analysis data of PAC1

Elemental analysis	C	H	O	N	(C/H) atom	O/C atom
Surface atomic concentration* (%)	85.18		12.74	1.98		
Surface elemental analysis* (wt %)	81.55		16.24	2.21		0.15
Average elemental analysis (wt %)	96.04	0.46	2.77	0.72	17.4	0.02

* Measured by XPS

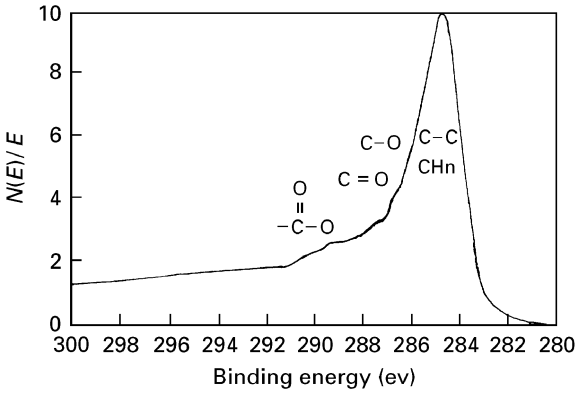

Figure 9 High energy resolution carbon 1 s XPS spectrum of PAC1.

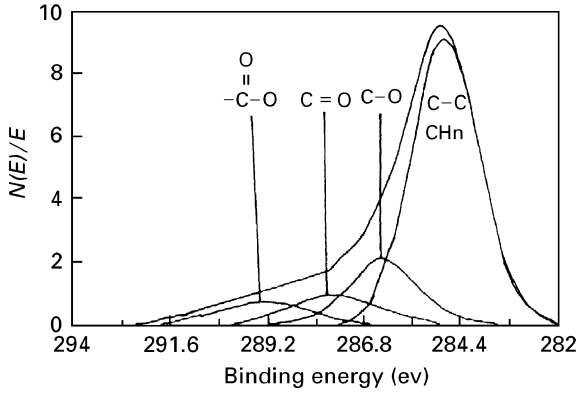

Figure 10 Fitted-carbon 1 s XPS spectrum of PAC1.

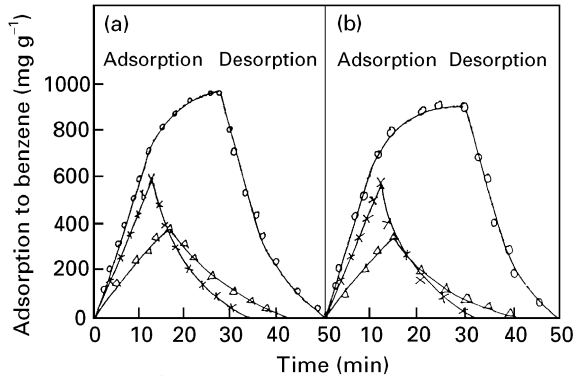

Figure 11 (a) 1st and (b) 2nd cycle adsorption–desorption behaviour of the samples to benzene vapour. (0) PAC1: $S_{BET} = 2666\,m^2\,g^{-1}$ (×) PACF: $S_{BET} = 2203\,m^2\,g^{-1}$, (△) AC: $S_{BET} = 1100\,m^2\,g^{-1}$.

less irreversible adsorption than AC and a good regeneration characteristic.

4. Conclusions

Pitch based activated carbon (PAC) with a surface area as high as $3600\,m^2\,g^{-1}$ could be obtained from infusible pitch by a chemical activation process using potassium hydroxide as the activation agent. PAC mainly consists of micropores with a radius around 0.5–2.0 nm, which results in a high adsorption–desorption velocity. It also has a large adsorption capacity due to its high surface area. The preparation conditions used had a strong influence on the final products, such as pore size and surface area. Another benefit of PAC is that the preparation process is quite simple although the oxidative stabilization of raw pitches takes a long time. Raw pitch could be shaped into a sphere before stabilization. Thus it appears that PAC is a new activated carbon, whose adsorption properties are in general superior to AC and even ACF.

References

1. J. WILSON, *Fuel* **60** (1981) 823.
2. B. McENANEY, *Carbon* **26** (1988) 267.
3. J. LAINE, A. CALAFAT and M. LABADY, *ibid.* **27** (1989) 191.
4. A. CHAKMA and A. MEISEN, *ibid.* **27** (1989) 537.
5. M. JAGTOYEN, M. THWAITES, J. STENCEL, B. McENANEY and F. DERBYSHIRE, *ibid.* **30** (1992) 1089.
6. P. J. M. CARROTT, R. A. ROBERTS and K. S. W. SING, *ibid.* **25** (1987) 59.
7. K. KANEKO and N. SHIDO, *ibid.* **27** (1989) 815.
8. W. M. QIAO, Q. F. ZHA, L. C. LING and L. LIU, *Carbon Techniques* (*China*) **3** (1994) 1.
9. *Idem*, in "Preparation and Properties of Pitch Based High Specific Surface Area Activated Carbon" Proceedings 22nd Biennial International Conference on Carbon, San Diego (1995) p. 400.
10. H. MARSH, D. CRAWFORD, T. M. O'GRADY and A. WENNERBERG, *Carbon* **20** (1982) 419.
11. A. WENNERBERG and T. M. O'GRADY, US Patent 4 082 694 (1978).
12. H. MARSH, D. S. YAN, T. M. O'GRADY and A. WENNERBERG, *Carbon* **22** (1984) 603.
13. T. OTAWA, M. SHIRAISHI, R. TANIBATA and N. TANAKA, in "Production and Adsorption Behavior of Maxsorb: High Surface Area Active Carbon", International Conference on Carbon, Essen, (1992) p. 944.
14. D. VALLADARES, S. MANZI, J. L. RICCARDA, J. MARCHESE and G. ZGRABLICH, in "Adsorption of CH_4 on Very High Surface Area Activated Carbon", International Conference on Carbon, Granada, (1994) p. 408.
15. G. C. GRUNEWALD and R. S. DRAGO, *J. Molec. Cataly*, **58** (1990) 227.

16. *Idem*, J. Amer. Chem. Soc. **113** (1991) 1636.
17. OTAWA, Y. NOJIMA and M. ITOH, in "Production and Adsorption Behavior of Maxsorb: High Surface Area Active Carbon", International Conference on Carbon, Granada, (1994) p. 808.
18. M. V. LOPEZ-RAMON, C. MORENO-CASTILLA, J. RIVERA-UTRILLA and R. HIDALGO-ALVAREZ, *Carbon* **31** (1993) 815.
19. S. J. GREGG and K. S. W. SING, "Adsorption, surface area and porosity," (Academic Press, New York, 1982).
20. E. DESIMONI, G. I. CASELLA and A. M. SALVI, *Carbon* **30** (1992) 521.
21. *Idem*, *ibid*. **30** (1992) 527.
22. R. H. BRADLEY, X. LING and I. SUTHERLAND, *ibid*. **31** (1993) 1115.
23. Z. Q. LUAN, M. R. ZHANG and K. X. CHEN, *ibid*. **31** (1993) 1179.
24. W. M. QIAO, Q. F. ZHA, L. C. LING and L. LIU, *Mater. Sci. Engng.* (*China*) **1** (1995) 41.
25. *Idem*, *Carbon* (*China*) **1** (1994) 1.
26. P. EHRBURGER, A. ADDON, F. ADDON and J. B. DONNET, *Fuel* **65** (1986) 1447.
27. K. KANEKO, C. ISHII, M. RUIKE and H. KUWABARA, *Carbon* **30** (1992) 1075.
28. L. C. LING, Y. H. SUN, L. LIU, M. Z. WANG and S. A. QIAN, in "Study on the Adsorption Behaviour of Pitch–Based Activated Carbon Fibre to Noble Metal Ion", International Conference on Carbon, Paris, (1990) p. 126.
29. T. J. BANDOSE, J. JAGIELLO, C. CONTESCU and J. A. SCHWARZ, *Carbon* **31** (1993) 1193.

Received 24 October 1995
and accepted 10 February 1997